RSC Advances

PAPER

View Article Online
View Journal | View Issue

Cite this: *RSC Adv.*, 2016, **6**, 39734

Functional organogelators formed by liquid-crystal carbazole-containing bis-MPA dendrimers†

I. Gracia,[a] J. L. Serrano,[b] J. Barberá[a] and A. Omenat*[a]

Received 15th March 2016
Accepted 14th April 2016

DOI: 10.1039/c6ra06835a

www.rsc.org/advances

Novel functional gelators with a dendritic structure based on flexible bis-MPA dendrons that combine mesogenic and carbazole moieties have been prepared. Both the precursory dendrons and the resulting codendrimers show rich supramolecular chemistry, exhibiting both liquid crystalline phases and gelling properties in several low-polarity organic solvents. The study of the self-assembly processes reveals that non-covalent weak interactions control the formation of the supramolecular gels. Due to the carbazole moieties, these gels show interesting electronic properties with an increased fluorescence emission arising from an aggregation-induced emission enhancement (AIEE) effect and electrochemical behaviour. Oxidative polymerisation has been proven to be effective for fixing the gel structure in thin layers of xerogels deposited on ITO electrodes.

Introduction

Due to their straightforward preparation, high functionality and versatility, gels have attracted a lot of interest during recent years in materials science, in fields such as electrooptics, sensors and organic electronics.[1–3]

Among supramolecular gels, dendritic molecules exhibit interesting properties that favour the formation of gel phases. A branched structure and the subsequent multivalency are the key features of these molecules that stand between low-molecular weight and polymeric gelators.[4–8] The tuning of the chemical structure of the core, the dendritic backbone or the peripheral units enables the formation of gels of different nature such as organogels, hydrogels or liquid-crystalline gels.[9] H-bonding interaction has been widely employed as the major driving force for the formation of self-assembled aggregates based on dendritic molecules because of its strength and directionality. Molecules functionalized with amino acids, peptides or other H-bond donor or acceptor motifs have been extensively studied to obtain dendritic gelators.[10–12] Self-assembly ruled by weaker interactions has been also explored by introducing aliphatic chains[13,14] or poly(benzyl)ether as repeating units.[15,16] In these materials, the dendritic effect can play an important role in the formation of supramolecular organisations.[17]

The introduction of π-conjugated structures in the backbone or the periphery of dendritic molecules has also been largely studied in optoelectronics because of the possibility to obtain self-organized functional materials with application as OLEDs, OPVs, OFETs and sensors.[18] The properties of these materials are often influenced not only by the structure of the molecules but also by their supramolecular self-assembly, which can lead to the modification of the emission properties. Aggregation usually causes the quenching of the fluorescence.[19–22] However, the reverse effect, known as aggregation induced emission enhancement (AIEE) effect, has also been described in some liquid crystalline or gel materials.[23–26] Recently, a highly efficient and versatile dendron with 2-(2′-hydroxyphenyl)benzoxazole at the core that can form stable organogels with various apolar and polar organic solvents has been developed. These fluorescent dendritic organogels exhibit gelation-induced enhanced fluorescence emission and multiple stimuli-responsive behaviour.[27]

Carbazole based gelators, and specially carbazole rigid dendrons,[28–31] have been widely studied because they usually show AIEE effect[32,33] which makes them good candidates as sensors towards fluoride ions or amine vapors[34,35] and some explosives, such as TNT.[36–39]

In our previous work, the synthesis of a family of block codendrimers that combine liquid crystalline and optoelectronic properties was reported.[40] Given the molecular structure of these macromolecules, the formation of a supramolecular network in the presence of an organic solvent can be envisaged, and will be favoured by intra- and intermolecular interactions between different regions of the molecules. These molecules are one of the few examples of codendritic organogels.[41,42]

In this paper, we focus on the study of the gelation properties of the dendrimers shown in Scheme 1.

[a]Dpto. Química Orgánica, Instituto de Ciencia de Materiales de Aragón-CSIC, Universidad de Zaragoza, 50009 Zaragoza, Spain. E-mail: aomenat@unizar.es
[b]Dpto. Química Orgánica, Instituto de Investigación en Nanociencia de Aragón, Universidad de Zaragoza, 50009 Zaragoza, Spain

† Electronic supplementary information (ESI) available. See DOI: 10.1039/c6ra06835a

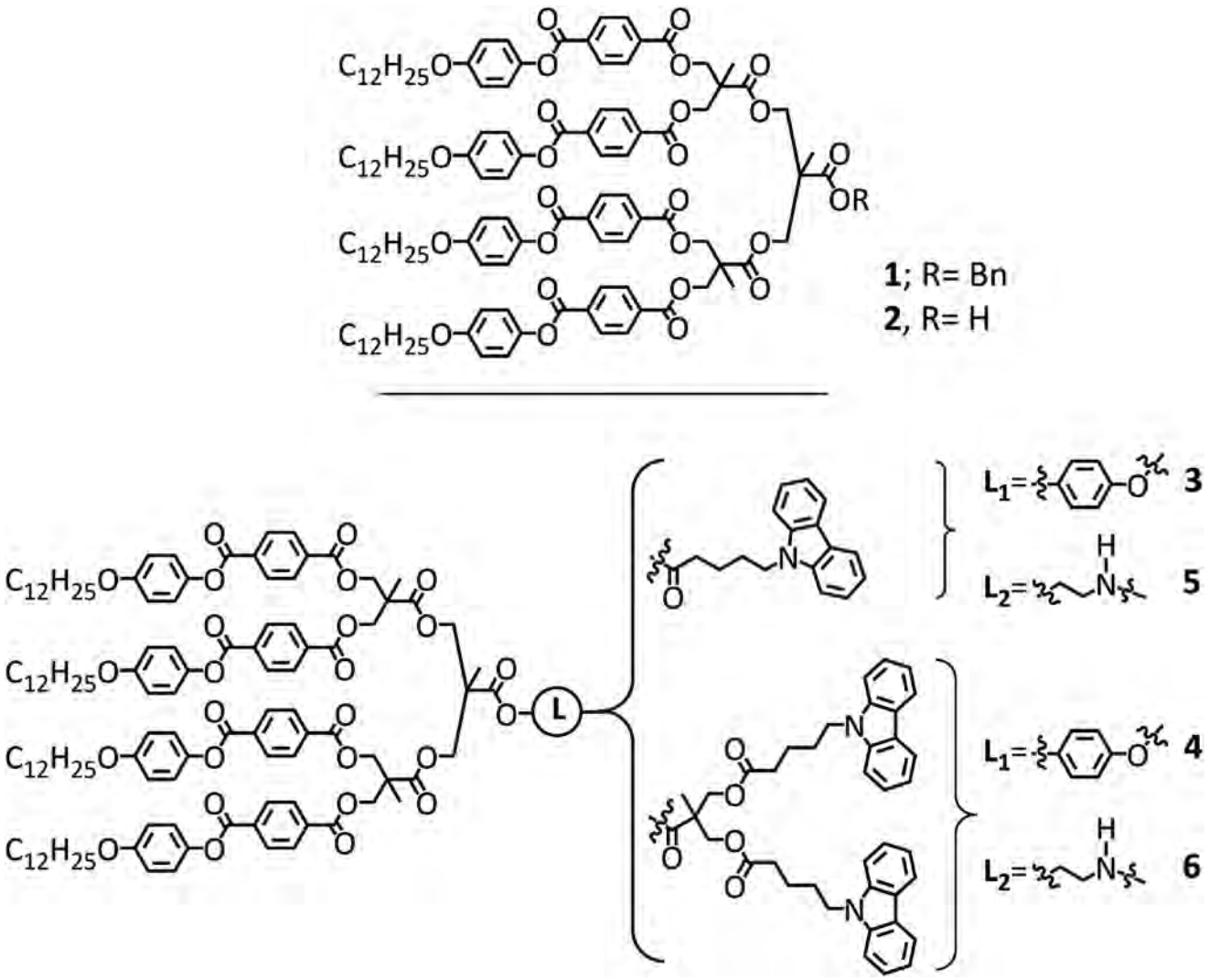

Scheme 1 Molecular structures of the dendrons and codendrimers studied.

Results and discussion

Synthesis

In an initial screening, it was found that dendrons and codendrimers with mesogenic units bearing just one dodecyloxy chain, directly linked to the periphery of 2nd generation bis-MPA dendrons, formed gels. Mesogenic bis-MPA dendrons **1** and **2**, and codendrimers **3** and **4** with a rigid linker (L_1) were already described in our previous work[40] (Scheme 1). Herein, **5** and **6** are prepared by condensation of **2** through a flexible linker (L_2) with the corresponding carbazole unit bearing one or two carbazole groups, respectively.

Liquid crystal properties

Liquid crystalline properties of the pure compounds were evaluated by POM, DSC and XRD. The results of these studies are gathered in Table 1. Block codendrimers **5** and **6** show an enantiotropic SmC phase. This statement is confirmed by POM observations (Fig. S1†). The structure of the mesophase is retained in the glassy state when the dendrimers are cooled down to room temperature. In comparison with the previously described monotropic phases of **3** and **4**, the introduction of a flexible linker between both dendrons in **5** and **6** with an amido group stabilises the mesophase by the enhancement of the intermolecular interactions by H-bonding, resulting in enantiotropic phases.

Powder XRD patterns of these compounds show a diffuse halo in the high-angle region corresponding to the short-range interactions between terminal aliphatic chains of the mesogenic dendron in the liquid crystalline phase. The low-angle region shows the first order reflection which denotes a lamellar packing (Fig. S2†). The characteristic structural parameter, *d* layer spacing, of the smectic packing was obtained by application of Bragg's law. These results are in good agreement with a cylindrical model in which two molecules of codendrimer associate to form a cylinder by interacting through their carbazole moieties while mesogenic units lie statistically upwards and downwards (Fig. S3†).[43,44] The similar values found

Table 1 Mesogenic properties and XRD data of the dendrons and codendrimers

Compound	Phase transitions[a]	T (°C)	Phase	d_{obs}[b] (Å)	Structural parameters[c] (Å^2)
1	C 34 [4.6] SmC 91 [10.8] I	rt	SmC(g)	33.5	$S = 207.2$ $S_{ch} = 51.8$
2	C 49 [11.2] C′ 130 [78.7] I [dec.][d]				
3	C 60 [12.5] C′ 120 [38.6] I I 113 [21.4] SmC 60 [14.0] C 39 [19.6] C′	80	SmC	37.3	$S = 208.5$ $S_{ch} = 52.1$
4	C 51 [21.4] I I 45 [15.6] SmC 19 C				
5	SmC(g) 33 SmC 46 [36.7] I	rt	SmC(g)	39.4	$S = 193$ $S_{ch} = 48$
6	SmC(g) 29 SmC 56 [27.5] I	rt	SmC(g)	43.5	$S = 203$ $S_{ch} = 51$

[a] Temperatures, read at the onset of the corresponding peaks, and enthalpies [KJ mol^{-1}, in square brackets] were obtained by DSC (second heating scan, 10 °C min^{-1}). C, C′ = crystal, SmC = smectic C mesophase, SmC(g) = glass maintaining the SmC order, I = isotropic liquid. [b] Measured layer spacing. [c] S = molecule cross-section and S_{ch} = cross-section per chain. [d] DSC values obtained in the first heating scan.

in all cases for the molecular cross-section and cross-section per chain (Table 1) supports this model. Differences between the lamellar constant and the theoretical length of the cylinder in the most elongated conformation of the molecules can be explained, apart from the conformational disorder, by the existence of interdigitation of the aliphatic chains of adjacent layers and also some degree of tilting in the mesophase expected for SmC mesophases.

Gel formation studies

The gel preparation procedures are detailed in the ESI.† A range of organic solvents were selected for the gelation tests. Non-polar or low-polarity solvents that can dissolve the compounds when temperature is slightly increased resulted to be the most effective gelation solvents (Table 2).

When polar or halogenated solvents were used alone, solubilisation occurred but no gel was formed afterwards, whereas in some very polar solvents, such as ethanol, or in long-chain hydrocarbons precipitation took place.

As seen in Table 2, the molecular structure plays an important role in the formation of the supramolecular assemblies. The introduction of an amido group in the linker between the mesogenic and the carbazole segments favours the gel formation (compare **5** and **3**) due to the increasing attractive interactions by H-bonding. The critical gelation concentration (CGC) for these compounds ranges from 1 to 0.25% wt. These low CGCs, specially for dendrons (**1** and **2**) and codendrimers bearing one Cbz group (**3** and **5**), are consistent with a strong dendritic effect,[9,16] which in this case means that the presence of four mesogenic units together enhances the stabilisation of the interactions through π–π and van der Waals forces. Thermoreversibility of the gels was stated in cyclohexane by measuring the gel–sol transition temperature (T_{gel}, in Table 2). As expected the T_{gel} values increase with the concentration (Fig. 1).

Moreover, it was also found that molecules with carbazole groups (dendrimers **3** and **5**) show lower T_{gel} values than those without them (dendrons **1** and **2**). This effect has already been observed in pure compounds where carbazole groups tend to prevent the formation of mesophases.[40]

The driving forces for the gel formation were evaluated by studying the dendrons **1** and **2** by NMR at variable temperature.

Table 2 Gelation tests and study of compounds **1–6** in several gelation solvents[a]

		Solvent[b]				
		Hex	Cy	Tol	Dod	1-Oct
Compound	**1**	I	**G** (0.5)[44]	S	**G**	**G**
	2	I	P	S	**G**	**G** (0.5)[60]
	3	I	**G** (0.5)[38]	S	P	**PG**
	4	I	**G** (1.0)[39]	S	P	**PG**
	5	I	**G** (0.25)[40]	S	**G**	**G**
	6	I	**G** (1.0)[38]	S	P	P

[a] G: gel, PG: partial gel, P: precipitate, I: insoluble, S: soluble. Critical gelation concentration (CGC, in wt%) in brackets and observed T_{gel} in square brackets. [b] Hex: *n*-hexane, Cy: cyclohexane, Tol: toluene, Dod: *n*-dodecane, 1-Oct: 1-octanol.

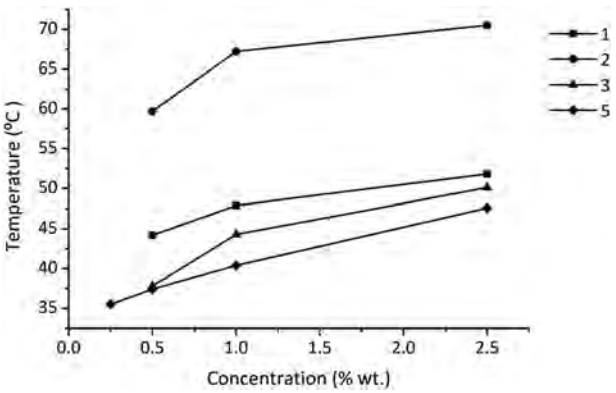

Fig. 1 Schematic representation of T_{gel} *vs.* concentration. All compounds measured in cyclohexane gels except **2**, which is measured in 1-octanol.

In the case of **1** only π–π, dipole–dipole and van der Waals interactions occur in the gel phase because all proton signals slightly shift to lower fields with increasing temperatures[45–47] (Fig. S4†). Once the carbazole unit is introduced to the mesogenic dendron, the ^{1}H NMR spectrum shows that the NH amide peak, at 6.1 ppm at 65 °C, is temperature dependent (Fig. S5†). This signal is shifted upfield (0.15 ppm) with increasing temperature, which is in accordance with the weakening of H-bonding with the temperature.

IR spectra also undergo important changes upon gelling in the N–H stretching band of **5** and **6,** that broadens and shifts from 3410 to 3555 cm^{-1} in **5** and almost disappear in **6** (Fig. S6†). In concentration dependent IR studies, we have also found that carbonyl bands shift to lower wavenumbers when decreasing concentration (Fig. S7†).

The morphology and structure of the gels were studied by SEM, TEM and XRD. SEM images usually show a layer of material resulting from the breaking of the structure upon evaporation of the solvent. However, for dendrons it is possible to observe bundles 500–800 nm thick formed by the association of 5 to 10 fibres (140–270 nm thick and 5–10 nm long), which are usually aligned along their long axis (Fig. S8†). The fibres found in samples of codendrimers are slightly thinner (70–100 nm) than those of dendrons and tend to aggregate in bundles that, in some cases, lead to the formation of ribbons. TEM observations show an interpenetrated network formed by fibres 23 ± 2 nm thick that associate in larger ribbons, as those observed by SEM (Fig. 2).

XRD studies of the xerogels carried out at room temperature confirmed a layered structure in the self-assembled systems (Table 3). Some of the diffractograms show a weak first order reflection at small angles while others only show weak higher order reflections in this angular region (Fig. S9†). These low-angle maxima are weak, whereas the high-angle diffuse halo is strong due to the majority presence of solvent.

Interlayer distances vary from those found for the SmC mesophases of the same compounds. The more functional groups able to participate in supramolecular interactions, the smaller interlayer distances are found.

In addition, π-interactions play an important role in the molecular packing in the gel phase as well. In this sense, the first generation dendrons of carbazole **4** and **6** tend to form more compact aggregates, which reduce the interlayer distances of the network compared to **3** and **5**, respectively, or to the precursory dendrons **1** and **2**.

Table 3 XRD data of the xerogels of compounds **1–6** in cyclohexane (2.5% wt)

Compound	d_{obs} (Å)	Reflection order	d_{calc} (nm)
1	41.1	001	4.1
2	20.0	002	4.0
	10.1	003	
3	40.0	001	4.0
4	18.3	002	3.7
5	18.6	001	3.7
6	18.0	002	3.6

All the data gathered from SEM, TEM and XRD allow us to suggest a molecular packing model in which fibres are formed by lamellae of 6 to 7 layers of gelling molecules (Fig. 3). The fibres form bundles of 70–270 nm thickness and the space between these fibres is filled by the molecules of the organic solvent. When concentration increases above the CGC, these bundles tend to aggregate in larger fibres or ribbons.

Optical properties and AIEE effect

Time dependent UV-Vis experiments show that in dilute solutions, no aggregation takes place and the absorption bands due to the n–π* electronic transition of carbazole at 332 nm remained unchanged.

However, in concentration-dependent experiments, those bands slightly red shift (Fig. S10†). Besides, when a warm solution was cooled to room temperature, it was possible to monitor the gel formation through the shifting of the UV-Vis signals. This same effect was observed in the fluorescence emission spectra. In this case, increasing the concentration and thus favouring the gel formation induces a bathochromic shift of the emission bands as well as the disappearance of the more energetic peak at concentrations close to the CGC (Fig. S11†). Interestingly, the extension of the aggregation with the time causes the increase of the intensity of the emission band without any shift in wavelength (Fig. 4).[48] These results confirm the slow process of gel formation and the AIEE effect.

Electrochemical polymerisation of xerogels derived from 5 and 6

The presence of the carbazole rings provides these systems with potential electrochemical behaviour. To evaluate the

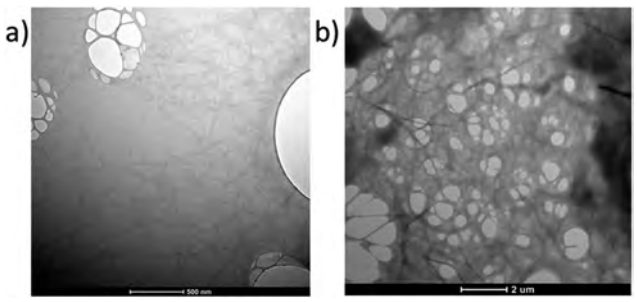

Fig. 2 TEM images of the dendritic aggregates formed in cyclohexane (0.1% wt): (a) compound **4**, (b) compound **6**.

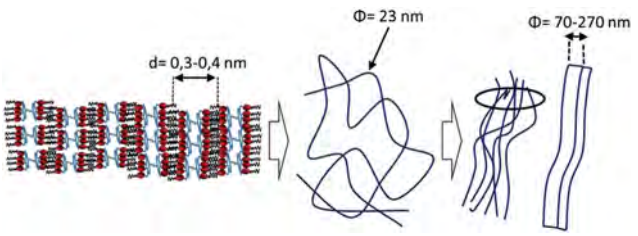

Fig. 3 Proposed model for the molecular packing in the gel phase.

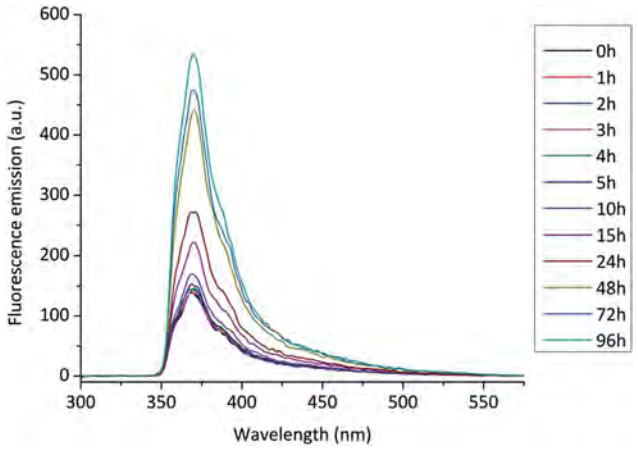

Fig. 4 Emission spectra of **6** in cyclohexane (0.17% wt) during the cooling and gel formation processes.

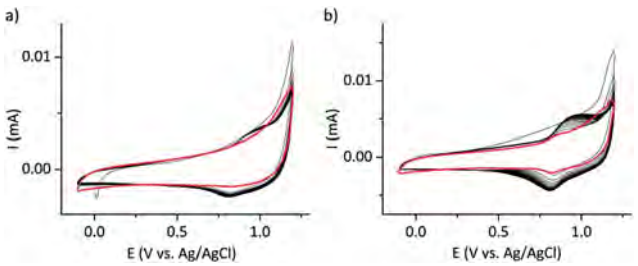

Fig. 5 CV traces for the electropolymerisation process xerogel-modified ITO-WE (black lines) (100 mV s^{-1}, 0.1 M $(n\text{-Bu})_4N(PF_6)$ in acetonitrile). CV traces of the electropolymerised materials (red lines): (a) compound **5**, (b) compound **6**.

electrochemical properties, we have prepared modified working ITO electrodes by coating the electrode surface with the cyclohexane gels of **5** and **6** and slow evaporation of the solvent to complete the xerogel formation.[49,50] These xerogel modified electrodes have been studied by cyclic voltammetry, using a three-electrode cell and acetonitrile as a solvent, in which **5** and **6** are insoluble. The CV studies have shown the electrochemical activity of these xerogels (Fig. S12†). In a further step, we have performed several scans on the same working electrode (WE) to provoke the electropolymerisation of the carbazole groups. Oxidative electropolymerisation effectively occurs in some extent as denoted by the increasing intensity and E_{pc} values of successive cycles (Fig. 5). The presence of more than one carbazole group per molecule favours the intra- and intermolecular crosslinking giving rise to a more extended chemical network. This material is less soluble in dichloromethane as shown by the voltammograms of the ITO electrodes after being soaked in this solvent.

The study of the electropolymerised ITO surfaces by SEM showed that a thin layer of the supramolecular self-assembled material is fixed during this process retaining the fibre nature of the xerogel in **5**, while an amorphous layer of material was obtained upon polymerisation xerogels of **6** (Fig. 6).

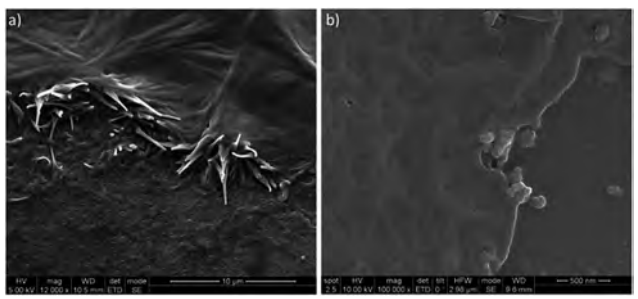

Fig. 6 FE-SEM images of electropolymerized xerogel films on ITO-WE: (a) compound **5**, (b) compound **6**.

Experimental

The general methods and materials as well as the synthesis of compounds **5** and **6** are gathered in the ESI.†

Gel and xerogel preparation

The procedure for the gel preparation consisted in weighing specific amounts of the different compounds and dissolving them in the corresponding volume of warm solvent until homogenous solutions were obtained. After slow cooling to room temperature, the solution gave rise to translucent or transparent gels in some of the cases. Precipitates or solutions were obtained in other. Gelation tests have been carried out starting with a 2.5% wt and decreasing 0.5% wt each time until no gel formation was observed. Gelling was investigated in all the cases by the inversion method,[51] and monitored over 72 hours. T_{gel} were estimated by heating the gels in a block-heater until they started to become fluid.

The xerogel samples were prepared by directly drop-casting the gel on a surface cleaned glass or ITO-electrode, and evaporating the solvent under vacuum at room temperature. For FE-SEM characterisation, xerogels were covered with gold. For TEM characterisation a drop of a solution 0.1% wt was deposited onto a copper mesh and allowed to dry at open air and stained with an aqueous solution of uranyl acetate (1% wt).

Conclusions

In conclusion, we have reported one of the first examples of multifunctional block codendrimer gelators that include a mesogenic dendron and a carbazole unit or dendron. It is remarkable that these molecules, **3–6**, show mesomorphic and gelling properties with different packing models for each supramolecular organisation. The use of carbazole as electronically active unit allows the combination of the aforementioned properties with the typical fluorescence emission and electrochemical behaviour of this π-conjugated group. Moreover, it has been proven that the prepared organogels have strong fluorescence-emission due to an aggregation-induced emission enhancement effect, which opens the possibility for the application of these dendritic gelators as sensors. The modification of a working-electrode with a xerogel and subsequent electropolymerisation has been accomplished, showing

that it is possible to fix the structure of the xerogel under certain conditions.

Acknowledgements

Financial support from the MINECO project CTQ2015-70174-P, and Diputación General de Aragón-Fondo Social Europeo (DGA-FSE) (Project E04) is gratefully acknowledged. I. G. acknowledges a MICINN-FPI fellowship. We thank the Laboratorio de Microscopías Avanzadas of the INA for the SEM and TEM and Nuclear Magnetic Resonance, Mass Spectrometry and Thermal Analysis Services from the CEQMA, Universidad de Zaragoza-CSIC (Spain).

Notes and references

1 A. Ajayaghosh, V. K. Praveen and C. Vijayakumar, *Chem. Soc. Rev.*, 2007, **37**, 109–122.
2 S. Diring, F. Camerel, B. Donnio, T. Dintzer, S. Toffanin, R. Capelli, M. Muccini and R. Ziessel, *J. Am. Chem. Soc.*, 2009, **131**, 18177–18185.
3 S. S. Babu, S. Prasanthkumar and A. Ajayaghosh, *Angew. Chem., Int. Ed.*, 2012, **51**, 1766–1776.
4 A. R. Hirst and D. K. Smith, in *Low Molecular Mass Gelator*, Springer, Berlin Heidelberg, 2005, pp. 237–273.
5 M. Seo, J. H. Kim, J. Kim, N. Park, J. Park and S. Y. Kim, *Chem.–Eur. J.*, 2010, **16**, 2427–2441.
6 R. Laurent and A.-M. Caminade, in *Dendrimers*, ed. A.-M. Caminade, C.-O. Turrin, R. Laurent, A. Ouali and B. Delavaux-Nicot, John Wiley & Sons, Ltd, 2011, pp. 267–311.
7 Y. Feng, Y.-M. He and Q.-H. Fan, *Chem.–Asian J.*, 2014, **9**, 1724–1750.
8 Y. Feng, H. Chen, S.-X. Liu, Y.-M. He and Q.-H. Fan, *Chem.–Eur. J.*, 2016, **22**, 4980–4990.
9 S. Chen, G. Tang, B. Wu, M. Ma and X. Wang, *RSC Adv.*, 2015, **5**, 35282–35290.
10 W.-D. Jang, D.-L. Jiang and T. Aida, *J. Am. Chem. Soc.*, 2000, **122**, 3232–3233.
11 E. R. Zubarev, M. U. Pralle, E. D. Sone and S. I. Stupp, *J. Am. Chem. Soc.*, 2001, **123**, 4105–4106.
12 G.-C. Kuang, X.-R. Jia, M.-J. Teng, E.-Q. Chen, W.-S. Li and Y. Ji, *Chem. Mater.*, 2012, **24**, 71–80.
13 C. Kim, S. J. Lee, I. H. Lee, K. T. Kim, H. H. Song and H.-J. Jeon, *Chem. Mater.*, 2003, **15**, 3638–3642.
14 C. Park, J. Lee and C. Kim, *Chem. Commun.*, 2011, **47**, 12042–12056.
15 V. Percec, M. Peterca, M. E. Yurchenko, J. G. Rudick and P. A. Heiney, *Chem.–Eur. J.*, 2008, **14**, 909–918.
16 Y. Feng, Z.-X. Liu, H. Chen, Z.-C. Yan, Y.-M. He, C.-Y. Liu and Q.-H. Fan, *Chem.–Eur. J.*, 2014, **20**, 7069–7082.
17 Y. Feng, Z.-T. Liu, J. Liu, Y.-M. He, Q.-Y. Zheng and Q.-H. Fan, *J. Am. Chem. Soc.*, 2009, **131**, 7950–7951.
18 S. S. Babu, V. K. Praveen and A. Ajayaghosh, *Chem. Rev.*, 2014, **114**, 1973–2129.
19 Y. Kamikawa and T. Kato, *Langmuir*, 2007, **23**, 274–278.
20 Y. Chen, Y. Lv, Y. Han, B. Zhu, F. Zhang, Z. Bo and C.-Y. Liu, *Langmuir*, 2009, **25**, 8548–8555.
21 A. Pérez, J. L. Serrano, T. Sierra, A. Ballesteros, D. de Saá and J. Barluenga, *J. Am. Chem. Soc.*, 2011, **133**, 8110–8113.
22 C. Romero-Nieto, M. Marcos, S. Merino, J. Barberá, T. Baumgartner and J. Rodríguez-López, *Adv. Funct. Mater.*, 2011, **21**, 4088–4099.
23 Z. Ning, Z. Chen, Q. Zhang, Y. Yan, S. Qian, Y. Cao and H. Tian, *Adv. Funct. Mater.*, 2007, **17**, 3799–3807.
24 Y. Hong, J. W. Y. Lam and B. Z. Tang, *Chem. Commun.*, 2009, 4332–4353.
25 R. Hu, N. L. C. Leung and B. Z. Tang, *Chem. Soc. Rev.*, 2014, **43**, 4494–4562.
26 J. Mei, Y. Hong, J. W. Y. Lam, A. Qin, Y. Tang and B. Z. Tang, *Adv. Mater.*, 2014, **26**, 5429–5479.
27 H. Chen, Y. Feng, G.-J. Deng, Z.-X. Liu, Y.-M. He and Q.-H. Fan, *Chem.–Eur. J.*, 2015, **21**, 11018–11028.
28 K. Yabuuchi, Y. Tochigi, N. Mizoshita, K. Hanabusa and T. Kato, *Tetrahedron*, 2007, **63**, 7358–7365.
29 X. Yang, R. Lu, T. Xu, P. Xue, X. Liu and Y. Zhao, *Chem. Commun.*, 2008, 453–455.
30 X. Yang, R. Lu, F. Gai, P. Xue and Y. Zhan, *Chem. Commun.*, 2010, **46**, 1088–1090.
31 Z. Ding, R. Xing, X. Wang, J. Ding, L. Wang and Y. Han, *Soft Matter*, 2013, **9**, 10404–10412.
32 Z. Yang, Z. Chi, T. Yu, X. Zhang, M. Chen, B. Xu, S. Liu, Y. Zhang and J. Xu, *J. Mater. Chem.*, 2009, **19**, 5541–5546.
33 W.-L. Gong, B. Wang, M. P. Aldred, C. Li, G.-F. Zhang, T. Chen, L. Wang and M.-Q. Zhu, *J. Mater. Chem. C*, 2014, **2**, 7001–7012.
34 D. Xu, X. Liu, R. Lu, P. Xue, X. Zhang, H. Zhou and J. Jia, *Org. Biomol. Chem.*, 2011, **9**, 1523–1528.
35 X. Liu, X. Zhang, R. Lu, P. Xue, D. Xu and H. Zhou, *J. Mater. Chem.*, 2011, **21**, 8756–8765.
36 T. Naddo, Y. Che, W. Zhang, K. Balakrishnan, X. Yang, M. Yen, J. Zhao, J. S. Moore and L. Zang, *J. Am. Chem. Soc.*, 2007, **129**, 6978–6979.
37 Z. Ding, Q. Zhao, R. Xing, X. Wang, J. Ding, L. Wang and Y. Han, *J. Mater. Chem. C*, 2012, **1**, 786–792.
38 P. Gong, P. Xue, C. Qian, Z. Zhang and R. Lu, *Org. Biomol. Chem.*, 2014, **12**, 6134–6144.
39 G. Hong, J. Sun, C. Qian, P. Xue, P. Gong, Z. Zhang and R. Lu, *J. Mater. Chem. C*, 2015, **3**, 2371–2379.
40 I. Gracia, B. Feringán, J. L. Serrano, R. Termine, A. Golemme, A. Omenat and J. Barberá, *Chem.–Eur. J.*, 2015, **21**, 1359–1369.
41 M. Yang, Z. Zhang, F. Yuan, W. Wang, S. Hess, K. Lienkamp, I. Lieberwirth and G. Wegner, *Chem.–Eur. J.*, 2008, **14**, 3330–3337.
42 M. Seo, J. H. Kim, J. Kim, N. Park, J. Park and S. Y. Kim, *Chem.–Eur. J.*, 2010, **16**, 2427–2441.
43 J. Barberá, B. Donnio, L. Gehringer, D. Guillon, M. Marcos, A. Omenat and J. L. Serrano, *J. Mater. Chem.*, 2005, **15**, 4093–4105.
44 M. Marcos, R. Martín-Rapún, A. Omenat and J. L. Serrano, *Chem. Soc. Rev.*, 2007, **36**, 1889–1901.
45 A. R. Hirst and D. K. Smith, *Org. Biomol. Chem.*, 2004, **2**, 2965–2971.

46 M. J. Clemente, P. Romero, J. L. Serrano, J. Fitremann and L. Oriol, *Chem. Mater.*, 2012, **24**, 3847–3858.
47 A. Pérez, D. de Saá, A. Ballesteros, J. L. Serrano, T. Sierra and P. Romero, *Chem.–Eur. J.*, 2013, **19**, 10271–10279.
48 S. Moyano, J. L. Serrano, A. Elduque and R. Giménez, *Soft Matter*, 2012, **8**, 6799–6806.
49 X. Yang, G. Zhang, D. Zhang and D. Zhu, *Langmuir*, 2010, **26**, 11720–11725.
50 P. Xue, Q. Xu, P. Gong, C. Qian, Z. Zhang, J. Jia, X. Zhao, R. Lu, A. Ren and T. Zhang, *RSC Adv.*, 2013, **3**, 26403–26411.
51 A. R. Hirst, D. K. Smith, M. C. Feiters, H. P. M. Geurts and A. C. Wright, *J. Am. Chem. Soc.*, 2003, **125**, 9010–9011.